In vitro study on human umbilical cord mesenchymal stem cells transfected with lentivirus-mediated hNIS-EGFP dual reporter gene and co-labeled with superparamagnetic iron oxide

YU MENG[1*], HUANHUAN LIU[1*], NING BIAN[2*], JIAN GONG[3], XING ZHONG[3], CHUNRONG HUANG[1], WENXUE LIANG[1] and HAO XU[1,3]

Departments of [1]Nephrology, [2]Cardiovascular Medicine and [3]Nuclear Medicine, The First Hospital Affiliated to Jinan University, Guangzhou, Guangdong 510630, P.R. China

Received April 30, 2016; Accepted May 5, 2017

DOI: 10.3892/etm.2018.6505

Abstract. The aim of the present study was to establish a stem cell line for multi-mode imaging (*in vivo* fluorescence imaging, magnetic resonance imaging and ^{99m}Tc single-photon emission computed tomography) and to study the biological activity, stemness, proliferative activity and differentiation ability of superparamagnetic iron oxide (SPIO), human sodium/iodide symporter (hNIS) and enhanced green fluorescent protein (EGFP) co-labeled human umbilical cord mesenchymal stem cells (hUCMSCs). The EGFP reporter gene was selected to indirectly reflect the expression of target gene hNIS, and hUCMSCs were re-transfected with the successfully constructed recombinant plasmid pCMV-NIS-EF1-GFP-PGK-puro. When a stem cell line stably expressing hNIS and EGFP was obtained, the cells were incubated with 30 μg/ml SPIO to obtain hNIS, EGFP and SPIO co-labeled stem cells. The protein expressions of hNIS and EGFP were identified using western blot analysis, and the protein function of hNIS was identified by ^{125}I influx and ^{125}I efflux experiments. hNIS-EGFP-hUCMSCs were labeled with SPIO under the mediation of poly-L-lysine, and SPIO, hNIS and EGFP co-labeled hUCMSCs were established successfully. Staining with Prussian blue confirmed that 98% of cells were successfully labeled with SPIO. Western blotting results demonstrated positive hNIS and EGFP protein expression levels, and ^{125}I influx and ^{125}I efflux experiments confirmed that the protein function of hUCMSCs after expressing hNIS was normal. The uptake of ^{125}I was higher in cell lines hNIS-EGFP-hUCMSCs than in control hUCMSCs (fold change: 16.43±2.30 times; $P<0.05$). The stemness of hNIS-EGFP-hUCMSCs was found to be slightly decreased but not statistically significant; the overall characteristics of stem cells remained unchanged. The assessments of adipogenic and osteogenic differentiation suggest that hNIS-EGFP-hUCMSCs have no significantly different characteristics compared with primary hUCMSCs.

Introduction

Mesenchymal stem cells (MSCs) have self-renewal capabilities and multi-directional differentiation potential, and are induced by different conditions to differentiate into various different tissues such as bone, cartilage, adipose, muscle, endothelial, epithelial and nerve tissue (1,2). MSCs may be used in transplantation for the treatment of systemic diseases, including leukemia, autoimmune disease and β-cell defects in diabetes (3). *In vivo* imaging technology may be used to dynamically observe the short-term distribution, homing and long-term survival of transplanted MSCs (4,5). The intravital tracer technique means that in stem cell transplantation, cells are able to be dynamically monitored *in vivo* to assess their migration and survival non- invasively (6-8). To obtain high definition images with high sensitivity, tracer technology for stem cells should be combined with multi-mode imaging (9). It is therefore of interest to establish a stem cell line with multi-mode imaging function. Generally, stem cell engineering studies require genetic modification of stem cells. At present, the instruments typically used to modify genes in mammalian cells include plasmid vectors, adenovirus vectors, retroviral vectors and lentiviral vectors (10). Lentiviral vectors are vectors for gene modification developed based on human immunodeficiency virus (HIV) (11). They are able to infect dividing and non-dividing cells, and integrate the target gene into the chromosomes of primary cells, stem cells and practically all cell types. Furthermore, the use of lentiviral vectors has few safety concerns and they are able to be expressed *in vivo* for a long time (12). These characteristics make the lentivirus vector an ideal instrument for gene modification (13,14). In

Correspondence to: Professor Hao Xu, Department of Nuclear Medicine, The First Hospital Affiliated to Jinan University, 613 Huangpu West Avenue, Guangzhou, Guangdong 510630, P.R. China
E-mail: xuhaodoc@163.com

*Contributed equally

Key words: human sodium/iodide symporter, enhanced green fluorescent protein, superparamagnetic iron oxide, mesenchymal stem cells

the present study, multiple labeling was performed for human umbilical cord mesenchymal stem cells (hUCMSCs) to enable them to be displayed using isotopic imaging, magnetic resonance imaging (MRI) and *in vivo* fluorescence imaging in order to establish effective *in vivo* tracer technologies, provide the basis for in-depth studies on hUCMSCs and enhance their homing ability.

Materials and methods

Extraction of hUCMSCs. hUCMSCs were obtained from umbilical cords harvested from 3 patients recruited to the Department of Obstetrics and Gynecology, the First Affiliated Hospital of Jinan University (Guangzhou, China) April to May 2013. The present study was approved by the Ethics Committee of the First Affiliated Hospital of Jinan University, and informed written consent was obtained from all patients from whom tissue was collected. Blood was removed from the blood vessels of the umbilical cord, and blood on the surface was washed off. The outer membrane of the umbilical cord was opened to excise veins and arteries, and hUCMSCs were harvested under aseptic conditions within 4-6 h of sample collection. Umbilical cord amniotic epithelium were removed to obtain Wharton's jelly, which were further dissected into ~1 mm^3 sections. The sections were incubated with 0.1% collagenase IV and digested at 37˚C for 24 h. The mixture was centrifuged at room temperature at 1,000 x g for 5 min. The pellet was resuspended with 0.1% trypsin and further digested for 30 min at 37˚C, and then was filtered through a 74 μm cell strainer. The filtrate was centrifuged at 1,500 rpm for 10 min. The cells were then completely resuspended and cultured in a 6-well plate at a density of $5x10^4$ cells/well in DMEM/F12 containing 2 ng/ml bFGF and 10% fetal bovine serum (all Gibco; Thermo Fisher Scientific, Inc., Waltham, MA, USA) at 37˚C under 5% CO_2 and relative humidity (100%). The culture solution was replaced 2 days later and the red blood cells and parenchyma cells that did not adhere to wall in the culture solution were removed. The culture solution was added again and became clear. Cellular morphology of hUCMSCs were observed every day under an inverted light microscope (Olympus CKX41; Olympus Corporation, Tokyo, Japan) at a magnification of x100 under normal culturing conditions.

hUCMSC identification and Induction of adipogenic and osteogenic differentiation. To confirm that the isolated and purified hUCMSCs were differentiated successfully, the following surface markers were selected: Cluster of differentiation (CD)73, CD90, CD105, hematopoietic stem/progenitor cell marker CD34, hematopoietic cell marker CD45. The expression of these markers was examined by flow cytometry. Briefly, a 50 μl cell suspension was seeded at a concentration of $2x10^7$ cells/ml in L-15 medium (Sigma-Aldrich; Merck MgaA). A total of 50 μl CD73 (cat. no. ab175396), CD105 (cat. no. ab49228), CD90 (cat. no. ab11153), CD34 (cat. no. ab185732), CD45 (cat. no. ab38436; all 1:500; all Abcam, Cambridge, UK) antibodies was added to the cells and incubated at 4˚C in dark for 30 min. The cells were then incubated with goat anti-rabbit immunoglobulin G (cat. no. ab6795; Abcam) as secondary antibodies at room temperature for 1 h. Wash cells by adding 2 ml L-15 and performing centrifugation for 5 min at 300 x g and room temperature. The stained cell pellet was resuspended in 400 ul L-15 at 4˚C and blocked by 5% skimmed milk at room temperature for 15 min. Flow cytometry analysis was conducted by CellQuest Software Pro 5.1 and a BD FACSVerse™ flow cytometer (both BD Biosciences, Franklin Lakes, NJ, USA). CD73, CD90, CD105 were highly expressed on the differentiated hUCMSCs, while CD34 and CD45 were barely detected on these cells.

The hUCMSC cells ($5x10^3$ cells) were seeded on 3 cm dishes in DMEM/F12 supplemented with 2 ng/ml bFGF and 10% FBS for 2 days. The cells were incubated with osteogenic or adipogenic differentiation media for 4 weeks. The adipogenic differentiation medium was composed of DMEM/F12 supplemented with 10% FBS, 100 nM dexamethasone, 50 μg/ml ascorbic acid and 50 μg/ml indomethacin. The osteogenic differentiation medium was composed of DMEM/F12 supplemented with 10% FBS, 10 nM dexamethasone, 10 mM β-glycerophosphate and 50 μg/ml ascorbic acid. As a negative control, cells were cultured in DMEM/F12 supplemented with 2 ng/ml bFGF and 10% FBS. Adipogenic differentiation was detected by Oil Red 'O' staining while osteogenic differentiation was detected by Alizarin Red-S staining as previously described (15) and digitalized for analysis using a Leica light microscope DMI3009B (Leica Microsystems GmbH, Wetzlar, Germany).

Construction of lentiviral vector

Obtainment of target gene human sodium/iodide symporter (hNIS). Expression plasmid pCMV-Tag2-hNIS preserved by the Central Laboratory at the First Affiliated Hospital of Jinan University was used. Primers were designed using Oligo 5.0 software (Molecular Biology Insights, Inc., Cascade, CO, USA) with reference to the hNIS-cDNA sequence registered in GeneBank (NM_000453.2). Upstream primer for NIS forward, 5'-GAATTCGCCACCATGGAGGCCGTGGAG AC-3' (EcoR I) and reverse, 5'-GCGGATCCTCAGAGGT TTGTCTCCTGCTGGTCTC-3' (BamH I), were synthesized by Sangon Biotech Co., Ltd. (Shanghai, China).

Purification of plasmid. A total of 4 plasmids pSico-enhanced green fluorescent protein (EGFP), pMDLg-pRRE, pRSV-REV and pMD2G were transformed. Briefly, 1 μg plasmid and 50 μl *E. coli* competent cells (Takara Biotechnology Co., Ltd., Beijing, China) were mixed in a 1.5 ml tube for 30 min at room temperature, then the tube was incubated at 42˚C for 90 sec. The tube was placed immediately on ice for 2 min. A total of 500 μl LB medium (Thermo Fisher Scientific. Inc.) was added to each tube, which was incubated for 1 h at 37˚C. Subsequently, 100 μl of the suspension was placed on a LB agar plate and incubated at 37˚C for 12-16 h. A fresh toothpick was placed on a colony, which was selected by adding streptomycin 50 mg/ml, kanamycin 50 mg/ml and ampicillin 60 mg/ml; the toothpick was then dipped into a 15 ml tube containing 3-5 ml super optimal broth (SOB) medium (Spectrum Laboratory Products, Inc., Shanghai, China). The tube was vigorously shaken at 37˚C (speed, 90 x g) for 8 h. The plasmids DNA used for transfections was prepared with the Endofree Plasmid Maxi kit (cat. no. 12362, Qiagen, Hilden, Germany) according to manufacturer's protocol.

Lentiviral titer determination. The 293T cells (Thermo Fisher Scientific. Inc.) were used for virus titer determination. Cells were inoculated in 96-well plates at a density of ~5x10^4 cells/well within 100 μl medium of DMEM containing 10% fetal bovine serum (FBS) at a 37˚C incubator with 5% CO_2. A total of 10 sterile eppendorf (EP) tubes containing 90 μl fresh medium of DMEM containing 10% FBS were used; 10 μl virus stock was added into the first EP tube and mixed well, and 10 μl solution was transferred from the first EP tube into the second. This process was repeated for the remaining tubes until the virus stock was diluted 10 times. A total 9 μl medium was removed from 10-well in the 96-well plate and 9 μl virus solutions from each of the prepared 10 tubes were added to each well, thus there were 5,000 cells in each well, and the concentration of the virus/well were 1, 10^{-1} and 10^{-2} μl, respectively. The cell culture plate was incubated at 37˚C in an atmosphere containing 5% CO_2 for 48 h. A total of 100 μl fresh medium was added into each well and incubation was resumed for 96 h. GFP fluorescence expression was subsequently observed under a fluorescence microscope and the number of fluorescing cells in the last two wells were counted.

Superparamagnetic iron oxide (SPIO)-labeling of hNIS-EGFP-hUCMSCs. hNIS-EGFP-hUCMSCs were incubated with SPIOs (50 μg; Biopal, Inc., Worcester, MA, USA). SPIO solutions were prepared at a 2x concentration in DMEM/F12 for 24 h. A total of 5 ml of 2x SPIO solutions were added to 5 ml of a hUCMSCs suspension in a 10 cm dish (5x10^4). The cells were plated on a 96-well plate, 100 μl for each, then 10 μl MTT was added to per well and incubated for 4 h, finally 100 μl DMSO solution was added per well until the formazan crystals dissolved, which was detected with 490 nm. Growth medium without SPIOs was added to sister cultures of hUCMSCs, these cells were used as the controls. Following incubation with SPIO, the cells were collected and washed twice in PBS; labeling efficiency was determined by Prussian Blue staining at room temperature for 30 min. The cellular morphology of hUCMSCs labeled with SPIO was observed under the inverted light microscope (Olympus CKX41, x400) for 8 days.

In vitro study of iodine uptake in transfected hUCMSCs. The experimental groups (SPIO-hNIS-EGFP-hUCMSCs) transfected with the lentivirus-hNIS-EGFP using the same kit and protocol as the 293T transfection. The control group (hUCMSCs) were untransfected cells. All groups were conventionally cultured and incubated in a 24-well plate at a density of 5x10^4 cells/well at 37˚C in an atmosphere containing 5% CO_2 overnight. When cells reached 80% confluence, the medium (DMEM/F12 containing 2 ng/ml bFGF and 10% FBS) was discarded and the cells were washed twice with Hank's Balanced Salt Solution (HBSS; Invitrogen; Thermo Fisher Scientific, Inc.). The ^{125}I uptake method was as previously described (16). Briefly, 1 ml HBSS (containing 0.1 μl of 100 uM sodium citrate ^{125}I) was added to each well and incubated at 37˚C for 30 min. The $NaClO_4$ inhibition test was conducted by incubation the cells with 300 μmol/l $NaClO_4$ for 60 min. This medium was discarded, cells were washed twice with cold HBSS, then cold 95% ethanol was then added to the cells and they were incubated at room temperature for 20 min. The concentrated iodide in the cytolysate was determined with a γ-counter (2480 WIZARD$_2$™ gamma counter; PerkinElmer, Inc., Waltham, MA, USA). The experimental and control groups each consisted of 6 independent wells in the 24-well plate.

Amplification of the hNIS gene. mRNA was extracted from the hUCMSCs using TRIzol and hNIS mRNA was amplified with one-step reverse transcription polymerase chain reaction (RT-PCR). The RT-PCR system solution was as follows: 20 μl of RNase Free dH_2O, 25 μl of 2x1 Step Buffer, 2 μl of PrimeScript 1 Step Enzyme Mix (Takara Biotechnology Co., Ltd.), 2 μl of upstream primers, 3 μl of downstream primers and 1 μl RNA samples. The primers were as follows: hNIS forward, 5'-CACCATGGAGGCCGTGGAG-3' and reverse, 5'-GAGGTTTGTCTCCTGCTGGTCTC-3'; β-actin forward, 5'-CTCCATCCTGGCCTCGCTGT-3' and reverse, 5'-GCTGTCACCTTCACCGTTCC-3'. The thermocycling conditions were as follows: 50˚C for 30 min, 94˚C for 2 min, 30 cycles of 94˚C for 30 sec, 50-65˚C for 30 sec and 72˚C for 1 min, and 72˚C for 10 min. The enzyme digestion system was: 1 μl 10X NEB-buffer, 0.5 μl EcorI, 0.5 μl xhol1, 5 μl PCR products/P3.1 vector (Hangzhou Xiaoyong Biotechnology Co., Ltd., Hangzhou, China) and 3 μl ddH_2O. The cells were then incubated with the digestion in 37˚C for 2 h prior to the PCR product was identified by 1% agarose gel electrophoresis, which was determined to have the same size as the target gene.

Colony PCR for recombinant plasmid. NIS gene segment and P3.1 vector were linked using the following protocol: 1 ul 10X buffer, 2 ul NIS gene segment, 4 ul P3.1 vector, 1 ul T4 ligase (Thermo Fisher Scientific, Inc.) and 2 ul ddH_2O were mixed overnight at 4˚C. The NIS gene segment and P3.1 vector was then transformed in complete medium (DMEM and 10% FBS) for 48 h at room temperature and coated on a LB medium plate without any antibiotics. Two monoclones were selected from the resistant plate with clear colony growth and amplified by PCR with Pn1 and Pn2 as the primers. The PCR product was identified by electrophoresis using a 1% agarose gel with ethidium bromide. The two monoclones revealed 1,900 bp gene segments, which was consistent with the theoretical value. It was preliminarily proven that these two colonies contained the correctly linked recombinant plasmids.

Screening of cell line stably expressing hNIS by puromycin. Determination of puromycin (Sigma-Aldrich; Merck KGaA, Darmstadt, Germany) screening concentration revealed that hUCMSCs were all killed following 7 days of exposure to 8 μl/ml puromycin. At concentrations <8 μl/ml, some hUCMSCs were not apoptosed; therefore 8 μl/ml was selected as the optimal puromycin screening concentration. hUCMSCs transfected with lentivirus were subsequently sub-cultured at a dilution of 1:10. When cell attachment occurred, 8 μl/ml puromycin was added to the medium. At 7 days following screening, positive cell colonies of hUCMSCs stably expressing hNIS and EGFP were obtained by screening with 8 μg/ml puromycin, and these were named as hNIS-EGFP-hUCMSCs and transferred to a 6-well plate for multiplication culture.

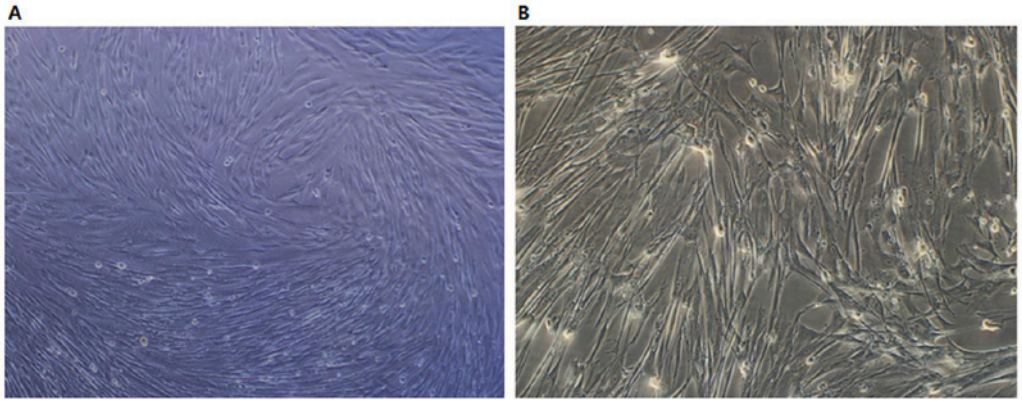

Figure 1. Cellular morphology of hUCMSCs. (A) Following 5 days of cell proliferation, hUCMSCs exhibited whirl or fingerprint-like growth (magnification, x100). (B) Sub-cultured hUCMSCs exhibited spindle-like growth (magnification, x200). hUCMSCs, human umbilical cord mesenchymal stem cells.

Identification of hNIS and EGFP expression in hUCMSCs using western blotting. Protein was extracted from $2x10^5$ cells using RIPA buffer (Thermo Fisher Scientific, Inc.) containing protease inhibitors (Roche Diagnostics, Basel, Switzerland). Protein concentration in the supernatants was measured using a bicinchoninic acid assay protein assay kit (cat. no. 23222; Thermo Fisher Scientific, Inc.). A total of 60 μg protein was transferred into an EP tube with 4X loading buffer and mixed well. The mixture was boiled for 10 min and centrifuged at 2,000 x g for 5 min. Proteins (10 μg/lane) were subsequently separated by 10% SDS-PAGE and transferred onto polyvinylidene fluoride membranes. Membranes were washed with Tris-buffered saline with 0.1% Tween-20 and blocked at room temperature in PBS with 0.1% Tween-20 (PBST) containing 5% skim milk powder for 1 h. Membranes were subsequently incubated at room temperature for 1 h with anti-hNIS (cat. no. ab83816; Abcam, Cambridge, UK), anti-EGFP antibodies (cat. no. 2956; Cell Signaling Technology, Inc., Danvers, MA, USA; both 1:3,000) and β-actin (cat. no. BM3501-01, 1:5,000; Biomiga, Inc., San Diego, USA) and washed with PBST. Membranes were incubated at room temperature for 2 h with the secondary horseradish peroxidase-labeled anti-Rabbit IgG (cat. no. ab191866; 1:10,000; Abcam), washed with PBST, then treated with SuperSignal West Pico Chemiluminescent Substrate (cat. no. 34077; Thermo Fisher Scientific, Inc.) for 1 h; the exposure time of X-ray film was 30 min. The membrane was washed with 0.5 mol/l NaOH for 15 min.

Statistical analysis. SPSS 13.0 (SPSS, Inc., Chicago, IL, USA) was used to perform statistic analysis. Experimental data are expressed as the mean ± standard deviation. Independent-samples t-tests were used to compare differences between groups. $P<0.05$ was considered to indicate a statistically significant difference.

Results

Morphological observation of hUCMSCs in vitro. Following 12 h of culture, the majority of hUCMSCs had adhered to the bottom of the plate and spread out gradually, with flat and spindle-like shapes and fibroblast-like growth. After five days of cell proliferation, confluence reached 80-90%, with cells distributed in clusters growing in a whirl or fingerprint-like manner (Fig. 1A). The sub-cultured hUCMSCs exhibited increased proliferative abilities and spindle-like growth (Fig. 1B). The cellular morphology of hUCMSCs after the third generation was uniform and cell growth entered plateau phase.

Expression of surface antigen of hUCMSCs by flow cytometry. Third generation hUCMSCs were identified by flow cytometry and they were found to be positive for CD73 (93.30%), CD90 (99.61%) and CD105 (99.06%); however, cells were negative for CD34 (0.80%) and CD45 (0.79%; Fig. 2), which was consistent with the phenotypic features of hUCMSCs.

Adipogenic induction for hUCMSCs

Cellular morphology. hUCMSCs were cultured with the adipogenic inducer and their appearance changed from spindle shaped to irregularly circular or polygonal, indicating clustering growth. At 4 days following the induction, intracellular circular lipid droplets were observed under the inverted microscope. Following continuous differentiation, the number of lipid droplets markedly increased and some fused to form large liquid droplets.

Oil red 'O' staining. At 28 days following adipogenic differentiation, third generation hUCMSCs were stained with oil red 'O'. Lipid droplets were observed to possess a red color in >80% of the cell with sharp contrast (Fig. 3A).

Osteogenic induction for hUCMSCs

Cellular morphology. Following osteogenic induction, the cellular morphology changed. On the fifth day of osteogenic induction, cell volume was observed to have increased and hUCMSCs exhibited short spindle-like or irregular polygonal shapes. Following continuous differentiation, hUCMSCs clustered and cascaded to form colonies. Calcified nodules were observed in the central regions and increased gradually.

Alizarin red staining. Following 4 weeks of osteogenic induction, third generation hUCMSCs were stained with alizarin red. Multiple black calcium nodules were observed at the central region of the cell colonies, which were stained black by reduced metallic silver (Fig. 3B).

Positive expression of hNIS-EGFP observed using fluorescence microscopy. Following transfection with EGFP

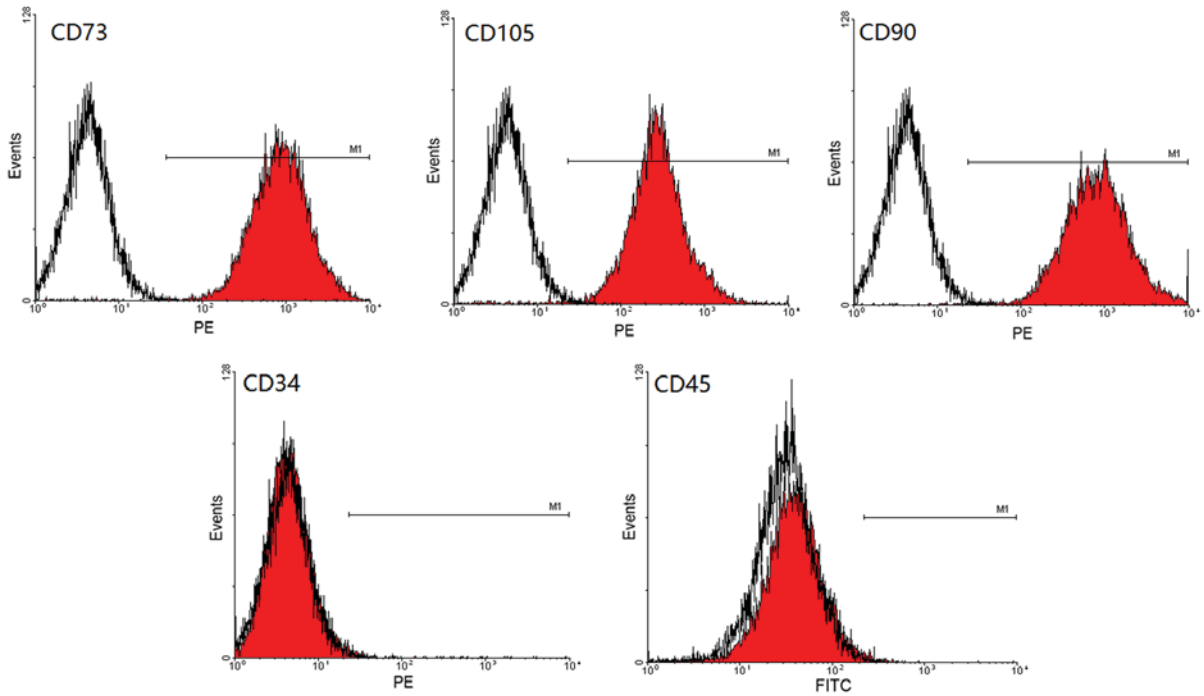

Figure 2. Expression of surface antigen of human umbilical cord mesenchymal stem cells determined by flow cytometry. PE, phycoerythrin; FITC, fluorescein isothyanicite.

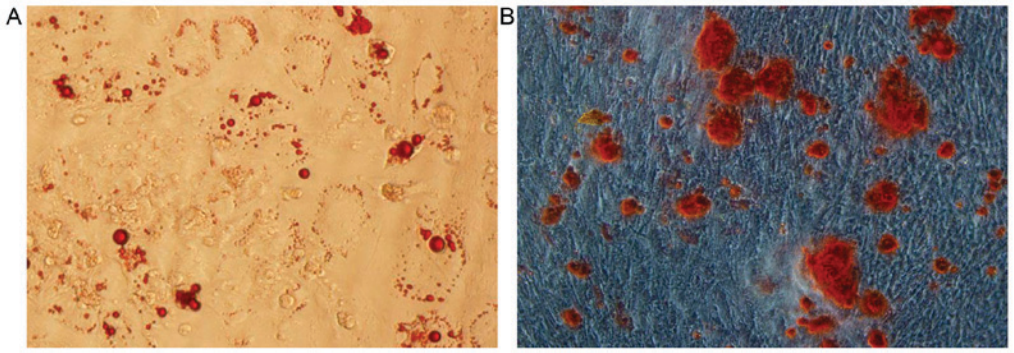

Figure 3. (A) At 28 days following adipogenic differentiation, the third generation hUCMSCs were stained with oil red 'O' (magnification, x200). (B) At 4 weeks following osteogenic induction, the third generation hUCMSCs were stained with alizarin red (magnification, x200). hUCMSCs, human umbilical cord mesenchymal stem cells.

and hNIS, the expression of hNIS in cells was assessed via fluorescence microscopy. At 12 h following transient transfection, a small number of hUCMSCs were observed to express green fluorescence with weak intensity. Following another 24 h, the number of fluorescing cells and the intensity of fluorescence increased, with 4-10/field in each field (magnification, x10). Over the subsequent 48 h, the number of human amniotic epithelial cells with green fluorescence increased continuously, with >10 in each field. No obvious differences were observed in the number of hUCMSCs with green fluorescence at 72 and 48 h. The majority of hNIS-EGFP-hUCMSCs fluoresced green under a fluorescence microscope (Fig. 4). It was observed that the virus infection efficiency for the NIS gene was >95%.

Identification of hNIS and EGFP expression in hUCMSCs by western blot. The cell lysate of the experimental (hNIS-EGFP-hUCMSCs) and control groups (hUCMSCs) underwent western blot analysis. Western blotting revealed positive bands at 90 kD (NIS) and 57 kD (eGFP) in the experimental group. Western blotting results for the control group did not reveal any specific bands (Fig. 5A).

SPIO-labeledhNIS-EGFP-hUCMSCs.hNIS-EGFP-hUCMSCs were co-incubated with SPIO again. It was confirmed by Prussian blue staining that SPIO transfection efficiency was >98%. The results are presented in Fig. 5B.

Study on cell biology of SPIO-labeled hNIS-EGFP-hUCMSCs Cell growth curve of hNIS-EGFP-hUCMSCs following labeling with SPIO. SPIO, hNIS and EGFP co-labeled hUCMSCs were sub-cultured. On days 1 and 2, hUCMSCs were latent and exhibited no marked proliferation. On days 3-7, hUCMSCs entered the logarithmic phase, and on days 7-8, hUCMSCs

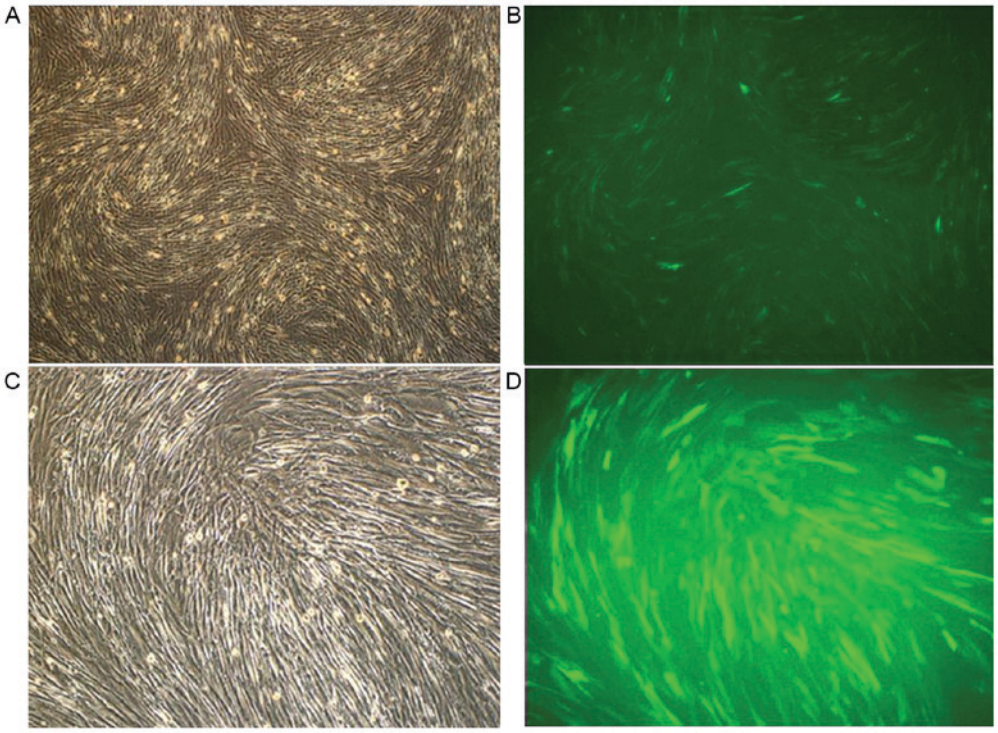

Figure 4. hNIS-EGFP-hUCMSCs with puromycin. (A) and (B) Day 3 following screening of hNIS-EGFP-hUCMSCs with puromycin (magnification, x100). (C) and (D) Day 7 following screening of hNIS-EGFP-hUCMSCs with puromycin (magnification, x200). hNIS, human sodium/iodide symporter; EGFP, enhanced green fluorescent protein; hUCMSCs, human umbilical cord mesenchymal stem cells.

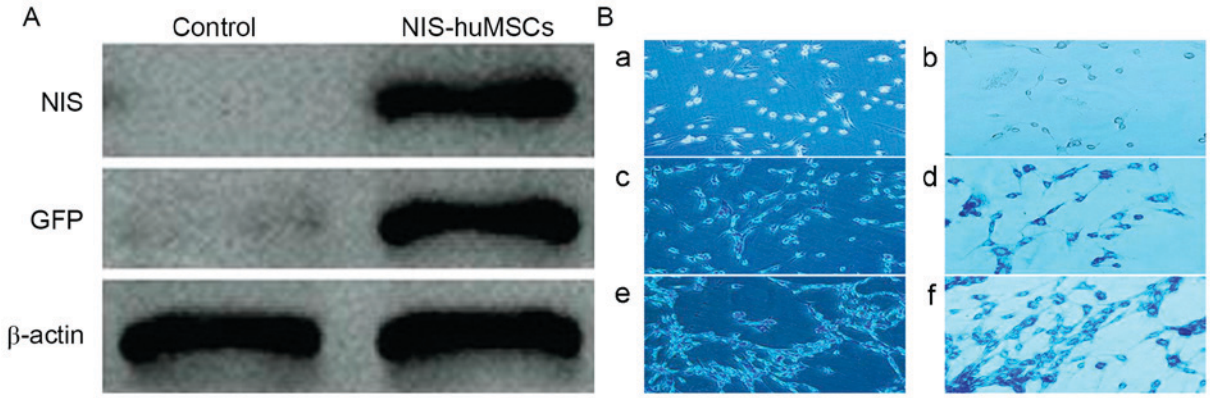

Figure 5. Western blot analysis and Prussian blue staining. (A) Identification of hNIS and EGFP expression in hUCMSCs by western blot analysis. *In vitro* study of ^{125}I uptake of hNIS-EGFP-hUCMSCs. (B) Prussian blue staining of superparamagnetic iron oxide-labeled hNIS-EGFP-hUCMSCs at (Ba and Bb) 0 h, (Bc and Bd) 24 h and (Be, Bf) 48 h. (magnification, x100). hUCMSCs, human umbilical cord mesenchymal stem cells; hNIS, human sodium/iodide symporter; EGFP, enhanced green fluorescent protein.

entered the plateau phase. Two double periods of cell growth were observed, the first on days 3-4 and the second on days 4-7. Compared with the control group (hUCMSCs), there was no significant difference in cell growth at any time point (Fig. 6A).

Adipogenic and osteogenic differentiation of hNIS-EGFP-hUCMSCs following labeling with SPIO. Experimental results demonstrated that modification with hNIS and EGFP and labeling with SPIO had no effect on adipogenic and osteogenic differentiation (Fig. 6B).

Phenotype identification of hNIS-EGFP-hUCMSCs following labeling with SPIO determined by flow cytometry. The adipogenic and osteogenic differentiation of normal MSCs and MSCs transfected with EGFP and SPIO were identified. The results revealed that the stemness of MSCs was not significantly decreased. Following transfection with EGFP and SPIO, and they were determined to be positive for CD73 (99.89%), CD90 (94.03%) and CD105 (91.94%) and negative for CD34 (0.13%) and CD45 (0.58%). There was no significant difference between the control and experimental groups (Fig. 7).

In vitro study on ^{125}I uptake of SPIO-labeled hNIS-EGFP-hUCMSCs. Uptake of ^{125}I was determined as previously described (17,18). ^{125}I uptake activity significantly increased by 16.43±2.30 times in the experimental group

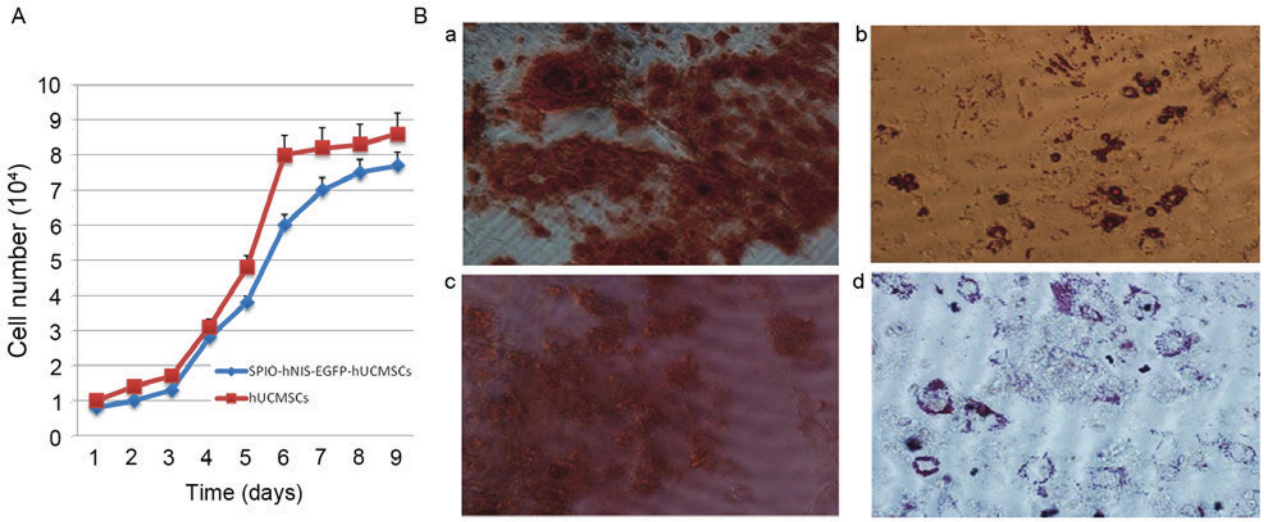

Figure 6. Cell growth curve and adipogenic and osteogenic differentiation. (A) Cell growth curve of hNIS-EGFP-hUCMSCs following labeling with SPIO. (Ba) Adipogenic and (Bb) osteogenic differentiation of hUCMSCs prior to labeling. (Bc) Adipogenic and (Bd) osteogenic differentiation of hUCMSCs following labeling (magnification, x200). hUCMSCs, human umbilical cord mesenchymal stem cells; hNIS, human sodium/iodide symporter; EGFP, enhanced green fluorescent protein; SPIO, superparamagnetic iron oxide.

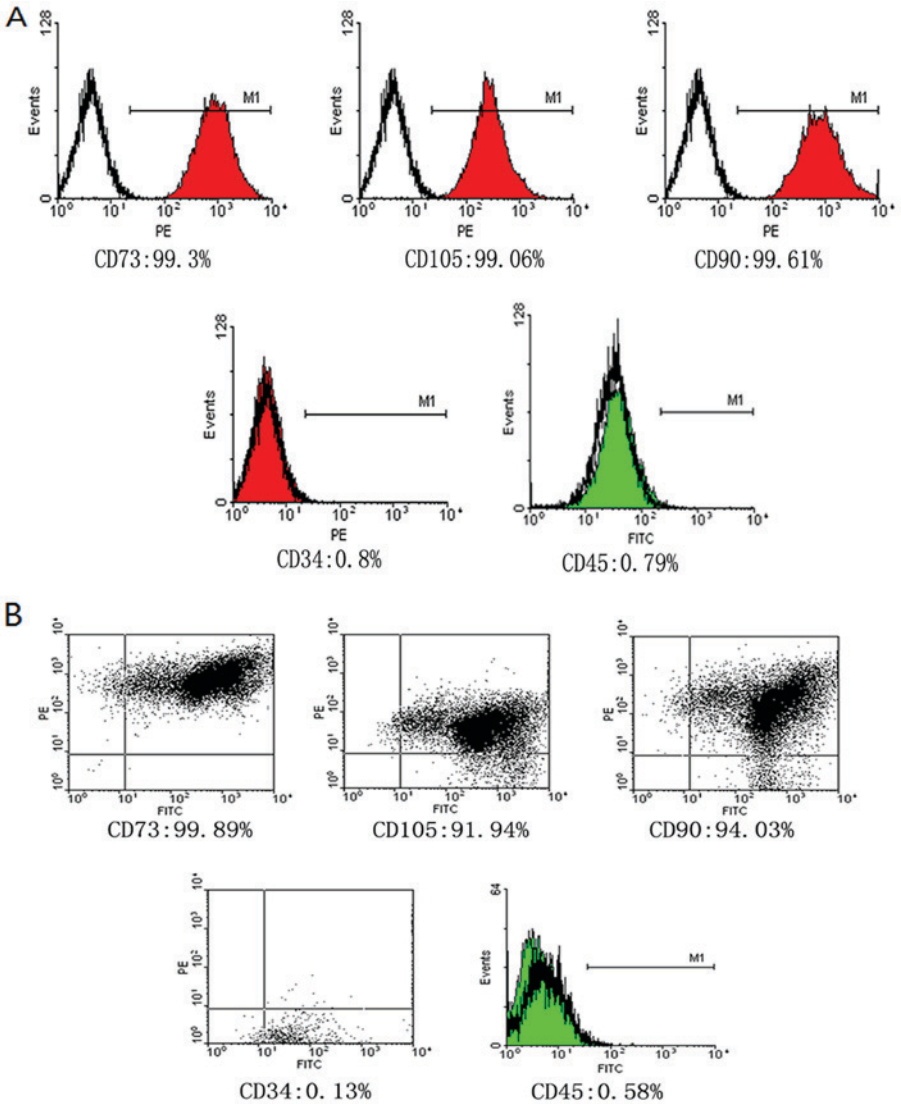

Figure 7. Phenotype identification of human sodium/iodide symporter-enhanced green fluorescent protein-labeled human umbilical cord mesenchymal stem cells following labeling with superparamagnetic iron oxide determined by flow cytometry. (A) Prior to and (B) following labeling. PE, phycoerythrin; FITC, fluorescein isothyanicite.

compared with the control group (P<0.05; Table I; Fig. 8A), accumulation was faster in SPIO-hNIS-EGFP-hUCMSCs than in hUCMSCs, reaching maximal levels within 30 min (Fig. 8B). The efflux of ^{125}I from SPIO-hNIS-EGFP-hUCMSCs was rapid, with half-maximal activity levels reached after 7.95 min (Fig. 8C).

Table I. ^{125}I uptake activity of superparamagnetic iron oxide-labeled human sodium/iodide symporter-enhanced green fluorescent protein-human umbilical cord mesenchymal stem cells.

Group	Without $NaClO_4$ (cpm)	With $NaClO_4$ (cpm)
Experimental	2005.2±52.0[a,b]	673.8.2±31.8
Control	122.7±20.9	98.3±10.5

[a]P<0.05 vs. the control group without $NaClO_4$; [b]P<0.05 vs. experimental group with $NaClO_4$.

Discussion

Compared with bone marrow mesenchymal stem cells (BMSCs), dental pulp stem cells (DPSCs), adipose derived stem cells (ADSCs) and embryonic stem cells (ESCs), hUCMSCs possess more primitive properties, strong plasticity and differentiation potential (19). Furthermore, hUCMSCs express the specific markers (CD73, CD90 and CD105) of stem cells (20). Compared with BMSCs, UMSCs have a greater proliferative ability, making them more suitable for clinical applications (21). Compared with ADSCs, hUCMSCs exhibit lower immunogenicity and no oncogenicity (22). hUCMSCs do not express human leukocyte antigen-antigen D related, which is a major causative factor of the immune response, suggesting that hUCMSCs may be suitable for transplantation between different individuals (23). Compared with other stem cells, the proliferative activity and differentiation ability of hUCMSCs does not decrease with sub-culture. Due to the aforementioned features, hUCMSCs were selected for use in the present study. Isotopic imaging, MRI and *in vivo* fluorescence imaging were compared or combined in order to identify effective *in vivo* tracer technologies, provide the basis for in-depth studies on hUCMSCs and enhance their homing ability.

hNIS is an endogenous gene derived from human thyrocytes, and its encoding product is a physiological protein that has no immunogenicity (24,25). The product of the hNIS reporter gene is expressed on the cell membrane, making it easier to capture the reporter probe compared with herpes simplex virus type 1 thymidine kinase and other reporter genes of intracellular enzymes (26). Endogenous hNIS is only expressed in certain tissues and organs, and commonly used radionuclides, such as ^{123}I and ^{99m}Tc may be used as reporter probes of hNIS; as such, there is no labeling requirement, which reduces the cost and increases accessibility (27). hNIS may be used for single-photon emission computed tomography (SPECT) or positron emission tomography and, as a reporter gene, hNIS is more stable than stomatostatin receptor 2 and human dopamine 2 receptor (28,29). However, the hNIS reporter gene lso has some deficiencies. As it is an endogenous gene, it is expressed in different degrees by several organs and tissues, such as the thyroid, gastric mucosa, mammary glands and salivary glands, which affects the monitoring of hNIS gene expression (30). In addition, in non-thyroid tissues and cells, iodine is released quickly because of a lack of thyroid specific proteins that hold iodine, therefore radioactive iodine does not accumulate (31-33). Although this reduces radiation damages to tissues, the signal detection is also affected.

For molecular biological techniques, the transfection of reporter genes into quiescent cells, in particular hUCMSCs, is difficult. The methods for transfecting target genes into target cells primarily include the transfection of eukaryotic expression plasmids and the transfection of viral vector-mediated genes (34). Studies on lentiviral vector (35) demonstrate that these vectors are able to effectively integrate exogenous genes into host chromosome to establish persistent expression (36). Lentiviral vectors are also able to effectively transfect neuronal, hepatic, myocardial, tumor, endothelial and stem cells (37). For cells that are difficult to transfect, such as primary, stem and non-dividing cells, the lentiviral vector increases the transduction efficiency of target genes greatly, allowing for the incorporation of RNAi, cDNA and study reporter genes (38). The lentiviral packaging system used in the present study is a four-plasmid system, consisting of pRsc-REV, pMD1g-pRRE, pMD2G and interference plasmid. The interference plasmid is able to express EGFP, pRsv-REV, pMDlg-pRRE and pMD2G, and contains the necessary elements for virus packaging (39). Eukaryotic plasmids containing the target gene, hNIS, were established and transfected with the aforementioned four-plasmids system to obtain hNIS-EGFP-hUCMSCs. Western blot analysis revealed that hNIS expression was normal. ^{125}I uptake activity of the experimental group (hNIS-EGFP- hUCMSCs) increased by 16.43±2.30 times in comparison with that of the control group (hUCMSCs). ^{125}I influx and efflux experiments indicated that the function of hUCMSCs was normal following the expression of hNIS, which indicates that it may be an effective reporter for SPECT *in vivo* cell tracing.

SPIO is a novel MR contrast, with a 20-200 nm diameter core of Fe_2O_3 coated with glucan (40). SPIO has very small crystal structures; under an applied magnetic field, SPIO exhibits single magnetic moment along the magnetic field (41). Even in a weak magnetic field, SPIO is highly magnetic (42). When the applied magnetic field is removed, this magnetism quickly subsides, and this is called superparamagnetism (43). Uneven distribution of SPIO in tissues results in an uneven local magnetic field (44), which shortens the transverse relaxation time (T2) and longitudinal relaxation time (T1) of tissues. The shortening of T2 is more marked, manifesting as the decrease in T2 signals (45). SPIO is negatively charged, and so in the present study, SPIO was coated with positively charged polylysine to reduce electrostatic interaction (29,32,33,46,47). Thus, SPIO was able to bind with cell surface receptors via electrostatic interaction and enter into cells via endocytosis. hNIS-EGFP-hUCMSCs are labeled with SPIO using the aforementioned technique,

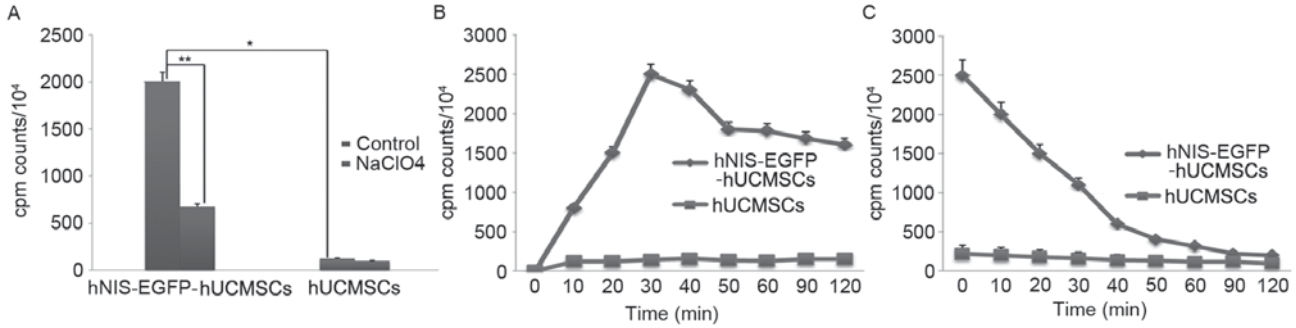

Figure 8. Dynamic process of ^{125}I. ^{125}I uptake activity of SPIO-labeled hNIS-EGFP-hUCMSCs. (A) ^{125}I uptake activity in the experimental and with the control group with and without $NaClO_4$. The (B) accumulation and (C) efflux of ^{125}I in the experimental and with the control group. $^{*}P<0.05$ and $^{**}P<0.01$. hUCMSCs, human umbilical cord mesenchymal stem cells; hNIS, human sodium/iodide symporter; EGFP, enhanced green fluorescent protein; SPIO, superparamagnetic iron oxide.

allowing for the successful establishment of SPIO, hNIS and EGFP co-labeled hUCMSCs. Staining with Prussian blue confirmed that SPIO entered cells, with a labeling rate of 98%.

The purpose of establishing SPIO, hNIS and EGFP co-labeled hUCMCs was to horizontally compare the advantages and disadvantages of several imaging technologies in *in vivo* stem cell transplantation. A series of tests were performed to determine whether the biological activity, stemness, proliferative activity or differentiation ability of hUCMSCs were affected following experimental interventions. On days 1 and 2 of sub-culture, hUCMSCs were at a latent phase with no obvious proliferation; on days 3-7, hUCMSCs entered the logarithmic phase, and on days 7-8, hUCMSCs entered the plateau phase. Cell growth had two double periods, the first on days 3-4 and the second on days 4-7. Compared with the control group (hUCMSCs), there were no significant differences at each time point. Adipogenic and osteogenic differentiation were further assessed prior to and following experimental treatments, and the experimental results suggest that the stemness of hNIS-EGFP-hUCMSCs was slightly reduced; however, the overall characteristics of stem cells remained unchanged. The results for adipogenic and osteogenic differentiation indicate that there are no significant differences between hNIS-EGFP-hUCMSCs and normal primary hUCMSCs. Western blotting also demonstrated that hNIS expression was good, and ^{125}I influx and ^{125}I efflux experiments indicated that the function of hUCMSCs was good following transfection with hNIS. These results suggest that hNIS-EGFP-hUCMSCs may be effective reporters for SPECT *in vivo* cell tracing. hNIS-EGFP-hUCMSCs were labeled with SPIO under the mediation of poly-L-lysine, and SPIO, hNIS and EGFP co-labeled hUCMSCs were successfully established. Staining with Prussian blue confirmed that SPIO successfully entered the cells, with a labeling rate of 98%. There were no significant differences in biological activity, stemness, proliferative activity or differentiation ability between SPIO, hNIS and EGFP co-labeled hUCMSCs and primary hUCMSCs. Therefore, the results of the present study suggest that, SPIO, hNIS and EGFP co-labeled hUCMSCs may be an effective treatment cell for animal models as it may be appropriate for stem cell tracing by SPECT, MRI and *in vivo* fluorescence imaging of animals.

Acknowledgements

Not applicable.

Funding

The present study was supported by grants from the Science and Technology Planning Project of Guangdong Province, China (grant nos. 2016A040403054 and 2013B021400002), Important Guangdong Province Science and Technology Specific Projects (grant nos. 2003A3080501 and 2015B010106008) and Important Industry-Academia-Research, Collaboration and Innovation Specific Projects of Guangzhou City (grant no. 201508020101).

Availability of data and materials

All data generated or analyzed during this study are included in this published article.

Authors' contributions

YM, HL and NB designed the experiment, established the lentivirus infection system, performed the statistical analysis and wrote the manuscript. JG processed and analyzed the single-photon emission computed tomography imaging. XZ provided plasmid of sodium/iodide co-rotor, designed the plasmid experiment and *in vitro* transfection. CH and WL performed magnetic resonance imaging scans and pathological research. HX guided the experiment, assisted with experiments where issues arose and reviewed the whole manuscript.

Ethics approval and consent to participate

Not applicable.

Patient consent for publication

Not applicable.

Competing interests

The authors declare that they have no competing interests.

References

1. Pittenger MF, Mackay AM, Beck SC, Jaiswal RK, Douglas R, Mosca JD, Moorman MA, Simonetti DW, Craig S and Marshak DR: Multilineage potential of adult human mesenchymal stem cells. Science 284: 143-147, 1999.
2. Crisan M, Yap S, Casteilla L, Chen CW, Corselli M, Park TS, Andriolo G, Sun B, Zheng B, Zhang L, *et al*: A perivascular origin for mesenchymal stem cells in multiple human organs. Cell Stem Cell 3: 301-313, 2008.
3. Tyndall A and Uccelli A: Multipotent mesenchymal stromal cells for autoimmune diseases: Teaching new dogs old tricks. Bone Marrow Transplant 43: 821-828, 2009.
4. Huang H, Zhang X, Hu X, Shao Z, Zhu J, Dai L, Man Z, Yuan L, Chen H, Zhou C and Ao Y: A functional biphasic biomaterial homing mesenchymal stem cells for in vivo cartilage regeneration. Biomaterials 35: 9608-9619, 2014.
5. Zhao C, Tian M and Zhang H: In vivo stem cell imaging. Open Nucl Med J 2: 171-177, 2010.
6. Ezzat T, Dhar DK, Malago M and Olde Damink SW: Dynamic tracking of stem cells in an acute liver failure model. World J Gastroenterol 18: 507-516, 2012.
7. Xia T, Jiang H, Li C, Tian M and Zhang H: Molecular imaging in tracking tumor stem-like cells. J Biomed Biotechnol 2012: 420364, 2012.
8. Schwarz M, Dörfler A, Engelhorn T, Struffert T, Tietze T, Janko C, Tripal P, Cicha I, Dürr S, Alexiou C, Lyer S: Imaging modalities using magnetic nanoparticles-overview of the developments in recent years. Nanotechnology Reviews 2013: 14, 2013.
9. Wolfs E, Holvoet B, Gijsbers R, Casteels C, Roberts SJ, Struys T, Maris M, Ibrahimi A, Debyser Z, Van Laere K, *et al*: Optimization of multimodal imaging of mesenchymal stem cells using the human sodium iodide symporter for PET and Cerenkov luminescence imaging. PLoS One 9: e94833, 2014.
10. Shearer RF and Saunders DN: Experimental design for stable genetic manipulation in mammalian cell lines: Lentivirus and alternatives. Genes Cells 20: 1-10, 2015.
11. Pavlovic M, Koehler N, Anton M, Dinkelmeier A, Haase M, Stellberger T, Busch U and Baiker AE: Reverse transcription quantitative polymerase chain reaction for detection of and differentiation between RNA and DNA of HIV-1-based lentiviral vectors. Hum Gene Ther Methods 28: 215-221, 2017.
12. Kantor B, McCown T, Leone P and Gray SJ: Clinical applications involving CNS gene transfer. Adv Genet 87: 71-124, 2014.
13. Hu YL, Fu YH, Tabata Y and Gao JQ: Mesenchymal stem cells: A promising targeted-delivery vehicle in cancer gene therapy. J Control Release 147: 154-162, 2010.
14. Gao Z, Zhang L, Hu J and Sun Y: Mesenchymal stem cells: A potential targeted-delivery vehicle for anti-cancer drug, loaded nanoparticles. Nanomedicine 9: 174-184, 2013.
15. Salehinejad P, Alitheen NB, Nematollahi-Mahani SN, Ali AM, Omar AR, Janzamin E and Hajghani M: Effect of culture media on expansion properties of human umbilical cord matrix-derived mesenchymal cells. Cytotherapy 14: 948-953, 2012.
16. Dwyer RM, Ryan J, Havelin RJ, Morris JC, Miller BW, Liu Z, Flavin R, O'Flatharta C, Foley MJ, Barrett HH, *et al*: Mesenchymal stem cell-mediated delivery of the sodium iodide symporter supports radionuclide imaging and treatment of breast cancer. Stem Cells 29: 1149-1157, 2011.
17. Zhong X, Shi C, Gong J, Guo B, Li M and Xu H: Experimental study of nasopharyngeal carcinoma radionuclide imaging and therapy using transferred human sodium/iodide symporter gene. PLoS One 10: e0117053, 2015.
18. Visser FW, Muntinga JH, Dierckx RA and Navis G: Feasibility and impact of the measurement of extracellular fluid volume simultaneous with GFR by 125I-iothalamate. Clin J Am Soc Nephrol 3: 1308-1315, 2008.
19. Riekstina U, Cakstina I, Parfejevs V, Hoogduijn M, Jankovskis G, Muiznieks I, Muceniece R and Ancans J: Embryonic stem cell marker expression pattern in human mesenchymal stem cells derived from bone marrow, adipose tissue, heart and dermis. Stem Cell Rev 5: 378-386, 2009.
20. Nan C, Shi Y, Zhao Z, Ma S, Liu J, Yan D, Song G and Liu H: Monosialoteterahexosyl ganglioside induces the differentiation of human umbilical cord-derived mesenchymal stem cells into neuron-like cells. Int J Mol Med 36: 1057-1062, 2015.
21. Ding DC, Chang YH, Shyu WC and Lin SZ: Human umbilical cord mesenchymal stem cells: A new era for stem cell therapy. Cell Transplant 24: 339-347, 2015.
22. Yang C, Lei D, Ouyang W, Ren J, Li H, Hu J and Huang S: Conditioned media from human adipose tissue-derived mesenchymal stem cells and umbilical cord-derived mesenchymal stem cells efficiently induced the apoptosis and differentiation in human glioma cell lines in vitro. Biomed Res Int 2014: 109389, 2014.
23. Dayem M, Basquin C, Navarro V, Carrier P, Marsault R, Chang P, Huc S, Darrouzet E, Lindenthal S and Pourcher T: Comparison of expressed human and mouse sodium/iodide symporters reveals differences in transport properties and subcellular localization. J Endocrinol 197: 95-109, 2008.
24. Zhou QB, Chen RF, Li ZH, Pan QH, Zhou JJ, Tang QB and Chen JS: Human mucin 1 promoter drives human sodium/iodide symporter gene targeting expression in pancreatic carcinoma cells. Zhonghua Yi Xue Za Zhi 87: 2780-2784, 2007 (In Chinese).
25. Han H, He W, Wang W and Gao B: Inhibitory effect of aqueous Dandelion extract on HIV-1 replication and reverse transcriptase activity. BMC Complement Altern Med 11: 112, 2011.
26. Che J, Doubrovin M, Serganova I, Ageyeva L, Beresten T, Finn R and Blasberg R: HSP70-inducible hNIS-IRES-eGFP reporter imaging: Response to heat shock. Mol Imaging 6: 404-416, 2007.
27. Merron A, Peerlinck I, Martin-Duque P, Burnet J, Quintanilla M, Mather S, Hingorani M, Harrington K, Iggo R and Vassaux G: SPECT//CT imaging of oncolytic adenovirus propagation in tumours in vivo using the Na//I symporter as a reporter gene. Gene Ther 14: 1731-1738, 2007.
28. Spitzweg C, Baker CH, Bergert ER, O'Connor MK and Morris JC: Image-guided radioiodide therapy of medullary thyroid cancer after carcinoembryonic antigen promoter-targeted sodium iodide symporter gene expression. Hum Gene Ther 18: 916-924, 2007.
29. Eekels JJ, Pasternak AO, Schut AM, Geerts D, Jeeninga RE and Berkhout B: A competitive cell growth assay for the detection of subtle effects of gene transduction on cell proliferation. Gene Ther 19: 1058-1064, 2012.
30. Serrano-Nascimento C, da Silva Teixeira S, Nicola JP, Nachbar RT, Masini-Repiso AM and Nunes MT: The acute inhibitory effect of iodide excess on sodium/iodide symporter expression and activity involves the PI3K/Akt signaling pathway. Endocrinology 155: 1145-1156, 2014.
31. Siddiqui F, Barton KN, Stricker HJ, Steyn PF, Larue SM, Karvelis KC, Sparks RB, Kim JH, Brown SL and Freytag SO: Design considerations for incorporating sodium iodide symporter reporter gene imaging into prostate cancer gene therapy trials. Hum Gene Ther 18: 312-322, 2007.
32. Bitsika V, Roubelakis MG, Zagoura D, Trohatou O, Makridakis M, Pappa KI, Marini FC, Vlahou A and Anagnou NP: Human amniotic fluid-derived mesenchymal stem cells as therapeutic vehicles: A novel approach for the treatment of bladder cancer. Stem Cells Dev 21: 1097-1111, 2012.
33. Nedeau AE, Gallagher KA, Liu ZJ and Velazquez OC: Elevation of hemopexin-like fragment of matrix metalloproteinase-2 tissue levels inhibits ischemic wound healing and angiogenesis. J Vasc Surg 54: 1430-1438, 2011.
34. Zhu Y, Cheng M, Lu N, Luo S, Xie Y and Liu D: Construction of NK4 gene lentiviral vector and its expression in bone mesenchymal stem cells. Sheng Wu Yi Xue Gong Cheng Xue Za Zhi 28: 976-981, 2011 (In Chinese).
35. Notka F and Wagner R: Reprogramming a GFP reporter gene subjects it to complex lentiviral gene regulation. Methods Mol Biol 813: 85-106, 2012.
36. Nethercott HE, Brick DJ and Schwartz PH: Derivation of induced pluripotent stem cells by lentiviral transduction. Methods Mol Biol 767: 67-85, 2011.
37. Buzon MJ, Erkizia I, Pou C, Minuesa G, Puertas MC, Esteve A, Castello A, Santos JR, Prado JG, Izquierdo-Useros N, *et al*: A non-infectious cell-based phenotypic assay for the assessment of HIV-1 susceptibility to protease inhibitors. J Antimicrob Chemother 67: 32-38, 2012.
38. Kim JE, Ahn BC, Hwang MH, Jeon YH, Jeong SY, Lee SW and Lee J: Combined RNA interference of hexokinase II and (131) I-sodium iodide symporter gene therapy for anaplastic thyroid carcinoma. J Nucl Med 52: 1756-1763, 2011.
39. Timmons CL, Shao Q, Wang C, Liu L, Liu H, Dong X and Liu B: GB virus type C E2 protein inhibits human immunodeficiency virus type 1 assembly through interference with HIV-1 gag plasma membrane targeting. J Infect Dis 207: 1171-1180, 2013.
40. Chen L, Altmann A, Mier W, Eskerski H, Leotta K, Guo L, Zhu R and Haberkorn U: Radioiodine therapy of hepatoma using targeted transfer of the human sodium/iodide symporter gene. J Nucl Med 47: 854-862, 2006.

41. Saraswathy A, Nazeer SS, Nimi N, Arumugam S, Shenoy SJ and Jayasree RS: Synthesis and characterization of dextran stabilized superparamagnetic iron oxide nanoparticles for in vivo MR imaging of liver fibrosis. Carbohydr Polym 101: 760-768, 2014.
42. Ittrich H, Peldschus K, Raabe N, Kaul M and Adam G: Superparamagnetic iron oxide nanoparticles in biomedicine: Applications and developments in diagnostics and therapy. Rofo 185: 1149-1166, 2013.
43. Hansen L, Hansen AB, Mathiasen AB, Ng M, Bhakoo K, Ekblond A, Kastrup J and Friis T: Ultrastructural characterization of mesenchymal stromal cells labeled with ultrasmall superparamagnetic iron-oxide nanoparticles for clinical tracking studies. Scand J Clin Lab Invest 74: 437-446, 2014.
44. Chao Y, Karmali PP and Simberg D: Role of carbohydrate receptors in the macrophage uptake of dextran-coated iron oxide nanoparticles. Adv Exp Med Biol 733: 115-123, 2012.
45. van Buul GM, Kotek G, Wielopolski PA, Farrell E, Bos PK, Weinans H, Grohnert AU, Jahr H, Verhaar JA, Krestin GP, *et al*: Clinically translatable cell tracking and quantification by MRI in cartilage repair using superparamagnetic iron oxides. PLoS One 6: e17001, 2011.
46. Levin MC, Lidberg U, Jirholt P, Adiels M, Wramstedt A, Gustafsson K, Greaves DR, Li S, Fazio S, Linton MF, *et al*: Evaluation of macrophage-specific promoters using lentiviral delivery in mice. Gene Ther 19: 1041-1047, 2012.
47. Sykova E and Jendelova P: In vivo tracking of stem cells in brain and spinal cord injury. Prog Brain Res 161: 367-383, 2007.